The 8th International Conference on Ubiquitous Robots and Ambient Intelligence (URAI 2011)
Nov. 23-26, 2011 in Songdo ConventiA, Incheon, Korea

Compliance Control of a Position Controlled Robotic Hand Using F/T Sensors

Joonhee Jo[1,2], Sung-Kyun Kim[1], Yonghwan Oh[1], Sang-Rok Oh[1]
[1]Interaction & Robotics Research Center, KIST, Seoul, 136-791, Korea
[2]Department of HCI & Robotics, UST, Daejeon, 305-350, Korea
(Tel : +82-2-958-5758; E-mail: {jhjo, kimsk, oyh, sroh}@kist.re.kr)

Abstract – There are a variety of robotic hands with many different hardware configurations including many sensors. For a robotic hand, physical interaction between the hand and objects is an interesting point. Compliance control is of great importance in grasping arbitrary object. In this paper, compliance control of position controlled robotic hand is attempted with external sensor on the finger tip. Utilizing an F/T sensor, sensor compensation first and then gravity compensation are executed. Overall system and algorithm are analyzed with the proposed controllers. For validating the proposed method, low-pass filter (LPF), sensor initial calibration are conducted and showed competent results.

Keywords – F/T Sensor, Compliance, Position Control, Robotic Hand.

1. Introduction

There have been many trials and diverse approaches on the research of robotic hand since 1950's. Mostly, a robotic hand has high degrees-of-freedom (DOF) and requires high level system modeling for control. In addition, for interaction with an object, expensive components such as force/torque sensors, tactile sensors, joint torque servo or current servo are imperative [1].

To configure a robotic hand, compliance control is a general issue in the manipulation hand for the safety problem. For controlling the robotic hand with the stable and safe movement, high performance servo motor for joint torque control and external sensors are on high demand. Joint torque servo can substantially improve the performance of a robotic system. However, the critical point is that components are too expensive to be configured for the robotic hand which is of over 12 -DOF. In addition, current servo has a difficulty in friction modeling though it can be alternative for joint torque servo. The higher spec components are used, the more costs are imposed. On this account, external sensor, which is less expensive than torque servo to be configured can be considered. F/T sensor on the fingertip is quite important for compliance control of position controlled the robotic hand.

While an external F/T sensor is necessary in hand configuration, it is too perturbed to use the sensor raw signals directly. Therefore, an F/T sensor which has a lot of noise needs to be compensated. Noises make sensor values oscillating and unstable, and result in incorrect controls of the hand. It is obvious that robot hand may break fragile objects with inappropriately compensated F/T sensor signals. Therefore, we use the low-pass filtering to get useful F/T values.

In addition to this, only noise filtering approach of compliance controlled robotic hand is not enough because of the gravity that affects the fingertip F/T sensor part. It is not ignorable enforcement and gravity compensation should be considered for a better compliance control. Additionally, gravity force has a different effect on the robotic hand according to the robot configuration. We consider gravity compensation for whole robot configuration. Therefore, we compute and convert the sensor values with respect to the sensor coordinate frame to those with respect to the base coordinate frame at every moment and apply them to input torque.

For the robotic hand which is operated by velocity mode, dynamics have to be computed and it is not easy and time consuming work. Hence, we approximate the velocities through impedance control [2, 3].

This paper proposes F/T sensor utilization for compliance control of a position controlled robotic hand. A calibration method of F/T sensor value is introduced in section 2, and synthesis of controllers in section 3. Moreover, for validating the proposed methods, set position compliance control experiments are presented in section 4 which includes robot configuration. At the end, section 5 concludes this paper.

2. Calibration of F/T Sensor at Fingertip

2.1 Low-Pass Filter

Figure 1 data is obtained with the external forces in the direction of x with respect to the sensor coordinate system as shown in Fig. 2. The measured data from the sensor is not as good as we can use directly, because the data contain a variety of noise by many factors such as improper groundings, white noise and so on. Some of noise is hardware noise which can be eliminated by adequate voltage ground and another is white noise which appears in every frequency band of the F/T sensor values. This noise can be eliminated by LPF, because most of signals which we are interested in are in low frequency region. We used a Butterworth third order low-pass filter to compensate sensor signal. Figure 1 shows frequency response of raw data whose noise which is not ignorant. Most of them are white noise which exists overall frequency region.

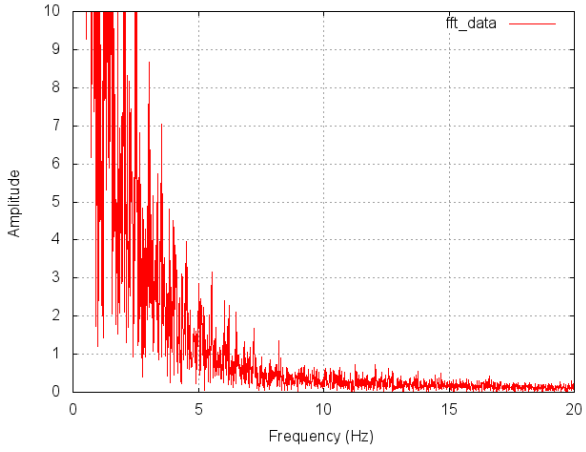

Fig. 1. FFT data analysis of x-axis F/T sensor signal with respect to the sensor frame in frequency domain.

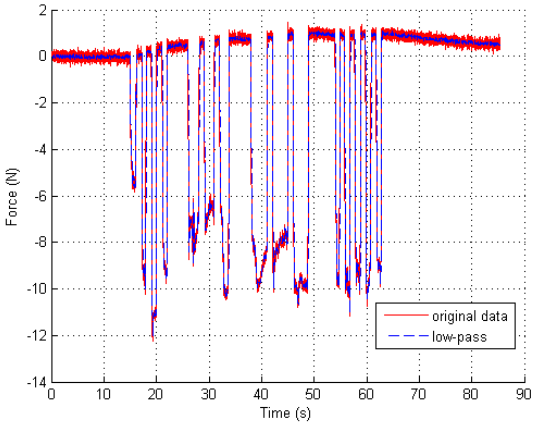

Fig. 2. Original data and filtered data are compared with respect to 10 Hz of cut-off frequency in the x-axis with respect to the sensor frame.

In Fig. 1, most of meaningful signals are within 10 Hz and others are noise. Thus, a cut-off frequency of the Butterworth is chosen as 10 Hz in Fig. 2 for the robot system based on the analysis for different frequencies. Solid line is the original data used in Fig. 1 which is not compensated and the dotted line is the data filtered by Butterworth third order LPF. When the cut-off frequency is 1 Hz, the filtered signal follows raw data slower than 5 Hz and so is 5 Hz than 10 Hz. Slower response means that you loss the data in real time. In the case of 15 Hz and 10 Hz, filtered data follows raw data quite well. However, 15 Hz is a little noisier than 10 Hz. No loss of data and less noise is important for the filter so that 10 Hz is the appropriate value for the cut-off frequency of LPF and as a result of that, you can see the data is filtered properly in Fig. 2.

2.2 Sensor Initial Calibrations

The sensor data have noise and some offset, so that they should be eliminated. 1000 samples of data are averaged at initializing stage to get the sensor offset. It should be noticed that the gravity effect by fingertip weight which is attached to the sensor is significantly involved during initial calibrations.

$$\frac{1}{N}\begin{pmatrix}\sum_{i=1}^{N} {}^{s}f_i \\ \sum_{i=1}^{N} {}^{s}m_i\end{pmatrix} = \begin{pmatrix}{}^{s}f_{avg} \\ {}^{s}m_{avg}\end{pmatrix} = \begin{pmatrix}{}^{s}\bar{f}_{offset} \\ {}^{s}\bar{m}_{offset}\end{pmatrix} + \begin{pmatrix}{}^{s}R_G & 0 \\ 0 & {}^{s}R_G\end{pmatrix}\begin{pmatrix}{}^{G}f_g \\ {}^{G}m_g\end{pmatrix} \quad (1)$$

${}^{s}f_i$ and ${}^{s}m_i$ are force and moment measured by the F/T sensor. ${}^{s}f_{avg}$ and ${}^{s}m_{avg}$ are averages of force and moment. ${}^{s}\bar{f}_{offset}$ and ${}^{s}\bar{m}_{offset}$ are the offsets of force and moment. ${}^{G}f_g$ and ${}^{G}m_g$ are the gravity force and moment. Superscripts of s and G stand for the reference coordinate frame of the sensor and the global one, respectively. In Eq. (1), all values are with respect to the sensor coordinate frame at time t = 0 which is an initial pose. The noise signal is not the only one included in the average data but also gravity term. This is because measuring part of sensor as well as fingertip part has a mass meaning that the dynamic effect by sensor part should be considered. The forces and moments by gravity are summed with the noise signals. Hence, when the noise signal is eliminated, it is necessary to take the gravity effects from the average values and offsets are obtained.

3. Synthesis of Controllers

3.1. Gravity Compensation using F/T Sensor

Fundamentally, fingertip position controller in section 3.2 doesn't consider external forces to the robotic hand but F/T sensor does. It is because an external force is not internal property of robotic hand.

For compliance control using F/T sensor, accuracy of f_{ext} in Eq. (2) is quite important. The exerted force on the fingertip is considered in the sensor frame.

$$\begin{pmatrix}{}^{s}f_{ext} \\ {}^{s}m_{ext}\end{pmatrix} = \begin{pmatrix}{}^{s}f_i \\ {}^{s}m_i\end{pmatrix} - \begin{pmatrix}{}^{s}\bar{f}_{offset} \\ {}^{s}\bar{m}_{offset}\end{pmatrix} - \begin{pmatrix}{}^{s}R_G & 0 \\ 0 & {}^{s}R_G\end{pmatrix}\begin{pmatrix}{}^{G}f_g \\ {}^{G}m_g\end{pmatrix} \quad (2)$$

Equation (2) shows pure external force and moment at arbitrary angle according to the robot configuration with the initial calibration force. In addition, because the torque input should be computed with respect to the robot base frame, the force/torque should change the reference coordinate system from sensor's to base frame through pre-multiplying ${}^{B}R_s$ which rotates from sensor coordinate system to base's. Calculated external force and moment through Eq. (2) are implemented to compliance control. To validate this method, experiments are conducted in section 4.

3.2. Task-Space Fingertip Position Compliance Controller

Compliance control of a position controlled robotic hand is the purpose of this paper. A first term of Eq. (3) which is the virtual spring-damper hypothesis is the basic controller of the system [4].

$$\tau = -J_p^T(q)(C\dot{e} + Ke) + J_p^T(q) f_{ext} + J_o^T(q) m_{ext} \quad (3)$$

where e is a task-space position error defined as $e = p - p_d$, and p_d is desired position of fingertip for the path planning with respect to the sensor frame. In addition, C is a positive definite diagonal matrix of damping coefficients, and K is a positive definite diagonal matrix of spring stiffness coefficients. Additionally, J_p^T and J_o^T are a position and an orientation Jacobian transpose to convert task space to joint space and τ is a torque input computed from position error. If a desired position is given, then desired torque to reach the position is computed by Eq. (3).

Since KIST-Hand is in the velocity control mode and each joint is assumed as 1st order system. Hence the robot controller computes the desired joint velocities by Eq. (4).

$$\dot{q} = \frac{\tau}{J_{eff} s + B_{eff}} \quad (4)$$

$\dot{q}$ is a velocity input computed from τ in Eq. (3) and J_{eff} is effective motor inertia defined as $J_{eff} = J_m N^2$ where J_m is a motor inertia and N is a gear ratio of harmonic drive. B_{eff} is an effective damping coefficient defined as $B_{eff} = B_m N^2$ where B_m is a motor damping coefficient. Originally, for computing the velocities, dynamics should be calculated for every moment. However computing dynamics requires expensive time cost. Hence, it is dealt with this problem by using effective inertia and damping to get velocities. With using this Eq. (4), the robotic hand still has a good accuracy for reasonably fast control period.

4. Experiment Result

The KIST-Hand is a multi-fingered dexterous robotic hand. It is consisted of four fingers with the thumb-fingers opposability. In addition, each four fingers have three DOF whose the third joint articulated by four-bar linkage at the fingers respectively except the thumb as shown in Fig. 3. The fourth joint linked to the cross four-bar linkage moves according to the third joint angle.

A force/torque sensor is installed at the fingertip for force feedback control used in KIST-Hand. The sensor is a tiny force sensor (TFS) made by NITTA Co., Japan. There is a calibration matrix to regulate the sensor signal. In addition, the sensor signal has +5 volts excitation from ground and it needs to be subtracted before being multiplied with the calibration matrix. Minute voltages for the calibrated sensor signal can be adjusted by variable resistors in the amp boards. Each amp board has 6 variable resistors for the voltage adjustment. Computation of

Table 1 F/T Sensor specification

Model		TFS12-25
Rating	Fx, Fy [N]	25
	Fz [N]	50
	Mx, My [$N \cdot cm$]	30
	Mz [$N \cdot cm$]	30
Measurement		Diaphragm gauge
Amp board voltage/current consumption		DC 12~15 V ripple P-P1, less than 0% / 47 mA
Sensor body weight		7 g

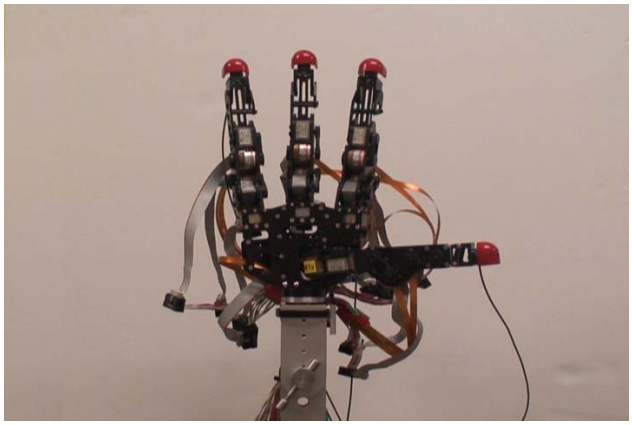

Fig. 3. KIST-Hand Configuration

calibration matrix produces a 6 by 1 vector whose first 3 by 1 vector is for the exerted force on the sensor and the rest of a 3 by 1 vector is for the torque. The calibration matrix is a transformation matrix from voltages to force and torque.

The maximum value of sensor measurement is different practically according to the coordinates. Among the values, we limit maximum value of 25 N for x and y-axis in Table 1 as a matter of safety. In addition, there is a DAQ PCI board which has 12-bit of resolution. Hence, the minimum force can be detected is 25 N / 4096 ≈ 0.0061 N. The change under 0.0061 N is neglected.

In the robotic hand, the controller should be operated within the regular time exactly. Real-time extension (RTX) is used for real time control in windows with 250Hz sampling rate. Every computation is fulfilled within the period. The KIST-Hand doesn't operate in the current mode but in the velocity mode. Because the joints are articulated by pulleys which cause loss of energy, it is quite difficult to use current mode.

4.1 Gravity Compensation

Since the compensations at the fingertip is already presented in the section 2 and 3, applying algorithms to the robotic hand and obtaining a competent result will be the main goal of this section. The experiment environment to validate the gravity compensation algorithm is shown up in the Table 2.

Actual weight of the whole sensor is 7 g. However, the measuring part on where external forces act is smaller than the whole body of the sensor. Assuming the weight of the

Table 2 Experiment environment

Sensor part weight	Assumed as 2 g
Sensor tip cover	16 g
The attached object	120 g

measuring part as 2 g, it is confirmed that the effect by this doesn't make a big difference in results.

$$0.002(Kg)\cdot 9.81(m/s^2) = 0.01962(N) \quad (5)$$

The result of Eq. (5) is very small portion of this experiment compared to Eq. (6) and Eq. (7). There exist limitations in gravity effect compensation. The fingertip and sensor measuring parts are modeled as point masses concerning static conditions only. With this inappropriateness, we obtained adequate results shown in Fig. 4. Figure 5 shows the robot thumb movement through angle changes.

We gave the robotic hand a change of second joint angle of the thumb from 80 to 60 degrees and to 40 degrees with the attached 120 g object. It means that a direction of external force changes in the x-z plane. This additional weight is for the higher contrast in results of gravity compensation. In Fig. 4, a dotted line is data before algorithm is applied and another after algorithm is applied is solid line.

As shown up in Fig. 4, when the algorithm is not applied, the enforcement changes according to the configuration of the robotic hand. The force changed when the second joint moved by 20 degrees from the initial position:

$$0.138(Kg)\cdot 9.81(m/s^2)\cdot \sin 80^\circ = 1.332(N) \quad (6)$$

$$0.138(Kg)\cdot 9.81(m/s^2)\cdot \sin 60^\circ = 1.171(N) \quad (7)$$

Equation (6) is the enforcement at initial position and Eq. (7) shows the ideal change of enforcement to the x-axis. Figure 5 shows the experimental result which is quite similar enforcement to the x-axis. So as to do for sure, we decrease the angle of second joint to 40 degrees.

$$0.138(Kg)\cdot 9.81(m/s^2)\cdot \sin 40^\circ = 0.869(N) \quad (8)$$

Obviously, there is a gravity effect on the F/T sensor due to the robot configuration change. Hence, this effect is necessary to be eliminated by gravity compensation algorithm. When the algorithm is applied, the enforcement to the x-axis is compensated so that the gravity effect by attached object is not shown in the solid line of Fig. 5. Despite the joint angle changes, compensated force shows complacent results.

4.2 Compliance Control

Applying compliance control to a robotic hand is our final goal in this paper. To validate the algorithms proposed in this paper, the algorithms are applied to KIST-Hand. As an experiment, set-point regulation for

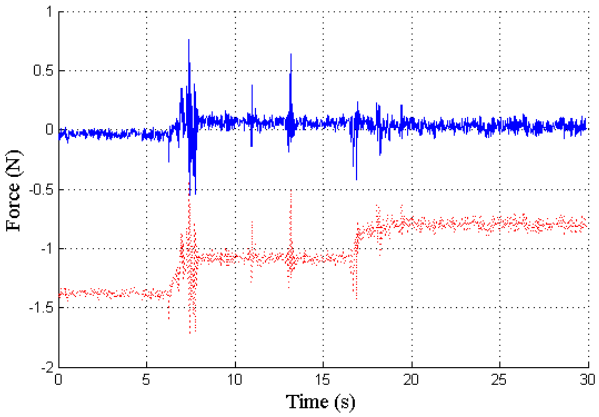

Fig. 4. Data comparison before (dotted line) and after (solid line) applying gravity compensation algorithm. The exerted forces on the F/T sensor are represented with respect to the robot base frame.

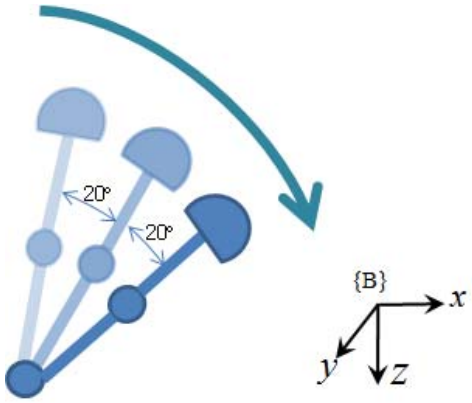

Fig. 5. Robot Thumb movement in x-z plane for gravity compensation experiment.

positions of the thumb under velocity control mode is used with the algorithms.

When the algorithms are applied, the thumb moves to the set position and is located in the desired position properly. Then, if there is a force in some direction through the F/T sensor, the thumb moves toward the direction of exerted force vector. In addition to this, if the external force is removed, the thumb moves toward the set position given before. The experimented data for the compliance control is displayed in Fig. 6. Solid line is the external forces which are exerted on the sensor and dotted line is the position of the end-effector of the robotic hand. Both of them are with respect to the robot base frame. The first exerted force is -x, +y and +z direction and another is +x, -y and -z direction with respect to the base frame. As Fig. 6 shows, the position follows the direction of force for all coordinates respectively. In addition, the cause that the exerted forces have a little bit of offset and slope is because of a modeling error and a drift of sensor itself.

Finally Fig. 7 shows that the robotic hand is of competent compliance control through the algorithms proposed in this paper.

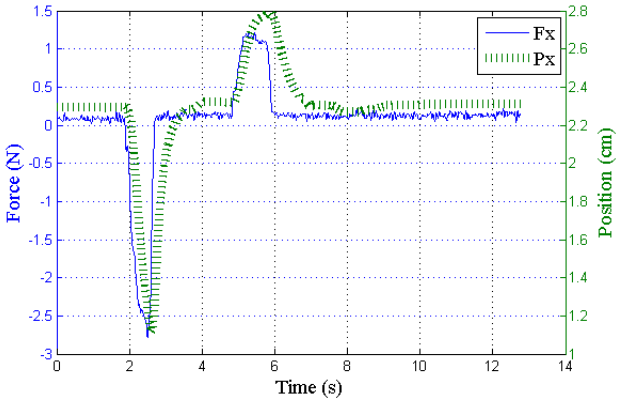

(a) X-axis

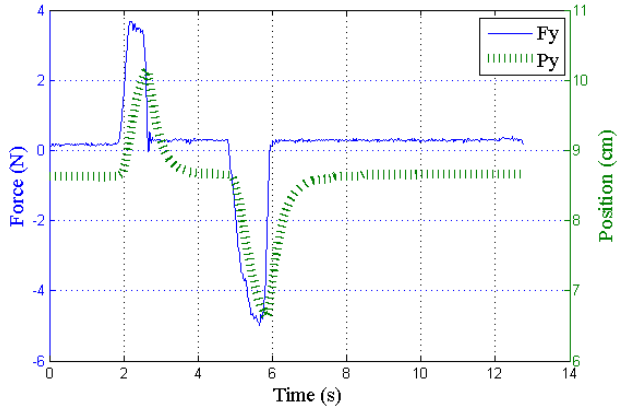

(b) Y-axis

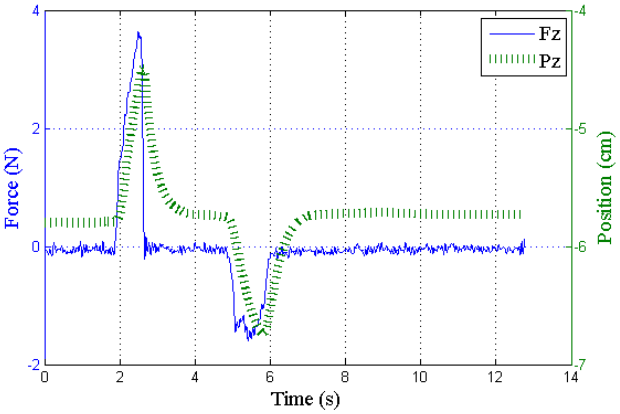

(c) Z-axis

Fig. 6. Force & position plot for the compliance control

5. Conclusion

The practical implementation of KIST-Hand is conducted in this paper. For utilizing F/T sensor, sensor weight initial calibration and sensor signal low-pass filtering are necessary for the proper sensor values. Through the compensations, complacent sensor values are obtained. In addition, task-space position controller is proposed based on compliance control and spring-damper hypothesis. Of great importance is compliance control which is applied through force feedback control with set position.

For the robotic hand, there are issues of grasping, pinching, gripping and so on. The controllers for these

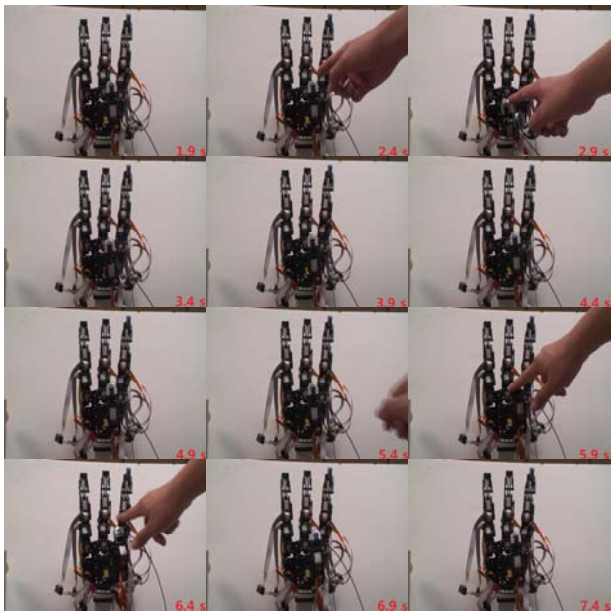

Fig. 7. Demonstration of compliance control

purposes require well-compensated signals in advance so that high accuracy can be guaranteed. Through this work, we have achieved competent results. Considerations on the fingertip inertia, force disturbance observer and grasping controls should be studied in future works.

References

[1] F. Ficuciello, *Modelling and Control for Soft Finger Manipulation and Human-Robot Interaction*, Ph. D dissertation, University of Naples Federico II, 2010.

[2] T. Valency, M. Zacksenhouse, "Instantaneous Model Impedance Control for Robots", *Proc. IEEE Int. Conf. on intelligent Robots and Systems*, vol. 1, pp. 757-762, 2000.

[3] Y.-J. Jung, *Grasping Force Control using Compliance-based Force normalization*, Master dissertation, Yonsei University, 2010.

[4] S.-K. Kim, B. J. You, Y. Oh and S.R. Oh, "Concurrent Control of Position/orientation of a Redundant Manipulator based on Virtual Spring-Damper Hypothesis", *Proc. IEEE Int. Conf. on Robotics and automation*, pp. 6045-6050, 2011.